Size Distribution Analysis for Copper Matte Particles Oxidized Under Flash-Converting Conditions

Manuel Pérez-Tello, José A. Tirado-Ochoa, Hong Yong Sohn, and Víctor M. Sánchez-Corrales

Mathematical correlations were developed to represent the size distributions of high-grade (72%) copper matte particles oxidized under flash-converting conditions in a large laboratory furnace. The correlation parameters for the oxidized particles were expressed as functions of the operating conditions in the furnace, namely, the mean size of the feed material and the oxygen-to-matte ratio. The statistical correlation parameter r^2 obtained with the mathematical expressions averaged 0.95 for the feed particles and 0.99 for the oxidized particles. The mathematical correlations were used to compute the amount of dust generated during the experimental runs. Good agreement between the correlated values and the experimental data was obtained. The potential application of the mathematical correlations for an industrial operation is discussed.

INTRODUCTION

The oxidation of sulfide particles at high temperatures is often accompanied by particle-size changes. Typical examples include the flash smelting of copper concentrates,[1] flash smelting of nickel concentrates,[2–4] and flash converting of copper mattes,[5,6] among others.[7] In these processes, particles change in size as a result of bloating followed by fragmentation in the reaction shaft. Although the reaction paths of individual particles in these processes are still under debate, qualitative models have emerged upon careful examination of particles reacted under controlled conditions.[8,9]

This article focuses on the flash-converting process of solid copper mattes.[10,11] In the flash-converting reactor, the magnitude of the size changes experienced by the particles is dependent upon their residence time in the reaction chamber and the operating conditions. Because the trajectories followed by individual particles vary from one particle to another, the size distribution of the particles at the bottom of the reaction shaft is that of a collection of particles with various histories and degrees of oxidation.

Particle-size measurements are of practical interest because they generate information that is relevant to dust generation in the flash-converting reactor. Dust is produced by particle fragmentation, and it causes a number of problems such as plugging of the transport system, corrosion, and a decrease in the steam production.[12–14]

The flash-converting reactor has been studied by the authors both experimentally in the laboratory[15] and computationally by means of a comprehensive three-dimensional fluid-dynamics model.[16] During the experimental work,[15] oxidation tests with low-grade (58%) and high-grade (72%) copper matte particles were done in a large laboratory furnace. Variables tested in the experiments included particle size of the feed material, oxygen-to-matte ratio, and oxygen concentration in the process gas. In the experiments, high-grade matte particles were observed to bloat and explode upon oxidation, thus producing large amounts of dust. Microscopic examination of the reacted particles suggested a reaction path similar to that proposed by Kim and Themelis[8] and further modified by Jokilaakso et al.[9] In contrast with the behavior of high-grade matte particles, the low-grade matte particles did not experience substantial changes in size under similar oxidizing conditions.

Based on the experimental observations, Swartling[17] developed a mathematical correlation for the size distribution of the particles upon oxidation in the laboratory furnace. The correlation parameters were expressed as functions of the variables tested in the experiments. The mathematical correlation was able to represent the cumulative distribution function of the particles with good accuracy (i.e., the mass fraction of particles in the population with sizes smaller than an arbitrary size x.) However, it failed to correlate the amounts of individual size fractions in the population. This was a serious limitation because the model could not compute the amount of dust generated in the experiments. Therefore, it was the purpose of this investigation to overcome this drawback by developing a new mathematical correlation capable of computing the relative amounts of individual size fractions in the population of particles before and after oxidation.

MATHEMATICAL CORRELATIONS

The goal of the correlations was twofold: to represent the size distributions of the reacted products collected in the bottom of the laboratory furnace, and to correlate the amount of dust generated in the experiments exactly.

Because the low-grade matte particles showed no significant size changes upon oxidation, the present study was based on the data collected with the high-grade matte particles only. High-grade matte particles are typically the feed material to the industrial flash-converting furnace;[10] thus, the study was justified in terms of its practical implications, as well.

In this study, the particle size distribution was expressed in terms of the mass-density function of the particle population, $f_3(x)$, which represents the mass fraction of particles in the

population within the size range [x, x+dx] divided by the range size dx. Integration of the density function yields the cumulative function, also called distribution function:[18]

$$F_3(x) = \int_0^x f_3(x')dx' \qquad (1)$$

The distribution function $F_3(x)$ represents the mass fraction of particles in the population with sizes smaller than x. From the above definitions the following relationship is obtained:

$$\int_0^{x_{max}} f_3(x')dx' = F_3(x_{max}) = 1 \qquad (2)$$

In the experiments,[15] the values of the density functions of both the feed and reacted particles were measured using a Microtrac technique, and the corresponding cumulative functions were computed from Equation 1. During the course of this study, it became clear that fitting the experimental values of the mass-density function $f_3(x)$ was a more difficult task than fitting the experimental cumulative-distribution function $F_3(x)$. However, fitting of the mass-density function $f_3(x)$ provided a detailed description of the size distribution of individual size fractions. Such information could not be correlated accurately by fitting the cumulative-distribution function, $F_3(x)$. Thus, the correlations were developed in terms of the mass-density functions, $f_3(x)$, and the corresponding cumulative functions $F_3(x)$ were computed numerically by doing the integration indicated in Equation 1. An outline of the general strategy is summarized as follows:

- Propose a mathematical function $f_3(x)$.
- Fit the experimental values of the mass-density function to the mathematical function $f_3(x)$- by means of a curve-fitting algorithm.
- Compute the statistical correlation parameter r^2 by means of the following expression:[19]

$$r^2 = 1 - \frac{\sum_{i=1}^{n} [g_3(x_i) - f_3(x_i)]^2}{\sum_{i=1}^{n} [g_3(x_i) - \overline{g_3(x_i)}]^2} \qquad (3)$$

  where $g_3(x_i)$ is the i-th experimental value of the mass-density function, $f_3(x_i)$ is the i-th value of the mass-density function predicted by the mathematical function, $\overline{g_3(x_i)}$ is the mean experimental value of the mass-density function, and n is the number of experimental data.
- Assess the mathematical correlation. A succesful mathematical correlation was assumed when the values of r^2 computed in step three was as close to unity as possible for all experimental data. If this criterion failed, the mathematical model was rejected and steps one through four were repeated.

For steps two and three, the curve-fitting capability built in a commercial software[20] was used. Once a satisfactory model was found, the values of the model parameters were correlated with the variables tested in the experiments.[15]

DISCUSSION OF RESULTS

During this study, efforts were made to obtain mathematical correlations based on the most common density function expressions reported in the literature.[18] Also, it was of interest to investigate whether the size distributions of both the feed and reacted particles could be represented by similar mathematical expressions, so that the oxidation process could be identified by differences in the parameter values. Therefore, the size distributions of the feed particles were correlated first, and the strategy outlined above yielded the following expression:

$$f_3(x) = bx^c e^{-ax} \qquad (4)$$

Equation 4 resembles the Gamma density function:

$$f_3(x) = (\lambda^n / \Gamma(n))x^{n-1}e^{-\lambda x}$$

in which $a = \lambda$, $c = n-1$, and $\Gamma(n)$ is the Gamma function of n. Parameter b in Equation 4 can be expressed as: $b = b_0(\lambda^n / \Gamma(n))$, where b_0 is a constant that depends on the experimental condition being fitted.

Table I shows the numerical values of the parameters for Equation 4 as well as the values of the correlation parameter r^2 obtained for all the size fractions in the feed. The correlation parameter r^2 averaged 0.95 for all the cases reported in Table I. The smallest value ($r^2 = 0.82$) was obtained for the <37 μm fraction. Figure 1 shows the fit obtained with Equation 4 for the <37, 74–105, and <149 μm fractions. The results for the 37–74 and 105–149 μm fractions were similar to those obtained with the 74–105 μm fraction, and thus are not shown.

Figure 1 indicates that the correlated values for the 74–105 and <149 μm feed fractions are in good agreement with the experimental data. Of particular interest is the <149 μm fraction, which represents the unsieved material with the widest size distribution. On the other hand, for the <37 μm fraction, in which the correlation parameter was the smallest ($r^2 = 0.82$), the correlation deviates somewhat from the experimental values. The <37 μm fraction contained the largest proportion of dust particles (<20 μm). It is of interest to note that despite the

Table I. Parameters for Equation 4

Size Range in the Feed Material (μm)	a	b	c	r^2
<37	0.0440	3.010^{-3}	0.8769	0.82
37 to 74	0.1346	8.710^{-12}	7.2224	0.99
74 to 105	0.1795	2.210^{-27}	16.3325	0.99
105 to 149	0.1549	3.5510^{-33}	18.6024	0.99
< 149	0.0252	3.6310^{-4}	1.1392	0.97

Figure 1. The correlated and experimental values of the particle size density functions in a selected number of feed fractions to the laboratory furnace. Experimental values are shown in geometric symbols; correlated values are represented by the continuous curves.

Table II. Parameters for Equation 5

Run No.	Particle Size Fraction in the Feed (μm)	Oxygen-to-Matte Ratio, kg O_2/kg mate	Oxygen Content in Process Gas (vol.%)	a_1 10^2	b_1 10^9	c_1	a_2 10^2	b_2 10^3	c_2	r^2
1	<37	0.25	70	6.38	7.89	4.284	6.23	5.81	0.527	0.998
2	<37	0.33	70	6.45	2.44	4.48	5.69	15.8	0.358	0.999
3	<37	0.25	100	7.48	0.8505	4.945	9.70	5.502	0.943	0.999
4	<37	0.33	100	5.31	75.7	3.52	8.24	13.55	0.444	0.999
5	37 to 74	0.25	70	10.6	0.0196	6.51	10.2	2.45	0.948	0.997
6	37 to 74	0.33	70	7.21	0.927	4.943	12.5	2.78	1.27	0.999
7	37 to 74	0.25	100	9.8	2.15×10^{-2}	6.338	7.56	3.47	0.652	0.998
8	37 to 74	0.33	100	7.45	5.35×10^{-4}	6.556	5.62	5.71	0.657	0.999
9	74 to 105	0.25	70	11.3	5.27×10^{-9}	10.09	9.39	3.03	0.811	0.995
10	74 to 105	0.33	70	9.96	3.02×10^{-7}	8.86	7.76	3.32	0.866	0.995
11	74 to 105	0.25	100	10.1	1.22×10^{-6}	8.65	11.3	1.71	1.09	0.985
12	74 to 105	0.33	100	7.61	1.30×10^{-6}	7.969	4.38	7.38	0.356	0.997
13	105 to 149	0.25	70	8.86	6.17×10^{-9}	9.51	5.63	6.02	0.382	0.984
14	105 to 149	0.33	70	9.33	4.03×10^{-12}	11.077	2.96	5.83	0.274	0.994
15	105 to 149	0.25	100	9.55	1.03×10^{-11}	11.0	3.03	5.59	0.204	0.994
16	105 to 149	0.33	100	8.82	1.54×10^{-10}	10.2	4.71	8.68	0.265	0.997
17	< 149	0.25	70	6.88	2.26×10^{-3}	6.28	4.06	1.68	0.479	0.994
18	< 149	0.33	70	8.64	6.52×10^{-4}	6.92	9.48	3.68	0.753	0.990
19	< 149	0.25	100	6.07	0.029	5.523	11.0	3.21	0.988	0.997
20	< 149	0.33	100	6.44	1.01	4.796	10.6	4.99	0.882	0.997

discrepancy between the correlated and the experimental values for this case, the amount of dust calculated in the feed using Equation 4 was in good agreement with the experimental data, as is discussed later in this article.

For the size distributions of the reacted particles, the following mathematical correlation was found to yield good results:

$$f_3(x) = b_1 x^{c_1} e^{-a_1 x} + b_2 x^{c_2} e^{-a_2 x} \quad (5)$$

This equation is an extended form of Equation 4 and it incorporates two terms on the right-hand side to represent the bimodal nature of the experimental data. Bimodal density function curves [i.e., the presence of two maxima in $g_3(x)$], were typically observed in the oxidized particles.[21]

The presence of two maxima in the size distribution $g_3(x)$ is the result of particle expansion and particle fragmentation occurring simultaneously in the reaction shaft. In the experiments,[15] the particle mean size decreased upon oxidation, which indicates that particle fragmentation dominated the overall process. Therefore, the two parts of the distribution in Equation 5 may be interpreted as the portion of the particles that largely retained the sizes in the feed and the portion that was generated by the particle break-up.

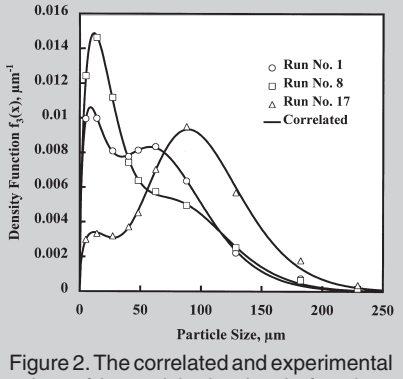

Figure 2. The correlated and experimental values of the particle size density functions in oxidized products in the laboratory furnace. Experimental values are shown in geometric symbols, and correlated values, by continuous curves. Experimental conditions according to Table II.

Table II shows the numerical values of the parameters for Equation 5 obtained for all the experimental conditions. The values of the correlation parameter r^2 are, in all cases, very close to unity, and they averaged 0.99. Figure 2 shows the fits obtained with Equation 5 for runs 1, 8, and 17, which are shown here as examples. Close agreement between the correlated and the experimental values is observed. This indicates that Equation 5 represents the experimental data well.

The use of Equation 5 requires the values of six parameters which, in turn, depend on the operating conditions tested in the laboratory furnace. Thus, it was of interest to express the correlation parameters as functions of the operating variables themselves. The parameters in Table II were fitted to a mathematical expression using a multivariate regression technique. By this procedure the following relationship was obtained:

$$p_j = \beta_{j,1}\bar{x}_f + \beta_{j,2}\bar{x}_f^2 + \beta_{j,3}R \quad (6)$$

In Equation 6, p_j is a general symbol for the j-th parameter in Equation 5, symbols $\beta_{j,1}$, $\beta_{j,2}$, and $\beta_{j,}$ are parameters obtained by the multivariate regression technique, R is the oxygen-to-matte ratio in kg O_2/kg of feed, and $\bar{x}_f$ is the mean size of the feed material in μm. Table III shows the definitions for the general symbols p_j used in Equation 6, the numerical values of the regression parameters $\beta_{j,1}$, $\beta_{j,2}$, and $\beta_{j,3}$, and the values of the correlation parameters r^2 obtained for Equation 6. Since closely screened fractions of the feed were used, except for the <37 μm and <149 μm fractions, the size spread of each fraction was small. It is of interest to note that even for these two feed samples with wide size distributions, the correlation using just the mean size without the spread yields good results as shown in Table III.

Equation 6 indicates that all the

Table III. Parameters for Equation 6

Parameter (p)	$\beta_1 \cdot 10^3$	$\beta_2 \cdot 10^5$	$\beta_3 \cdot 10^2$	r^2
a_1	1.9783	–0.91965	–3.8283	0.976
$b_1^{0.01}$	14.093	–7.6269	135.31	0.992
c_1	100.76	–14.935	–55.315	0.989
a_2	2.7388	–1.7770	–4.6342	0.922
b_2	–0.31676	0.17124	6.3218	0.874
c_2	31.976	–20.329	–139.83	0.912

Table IV. Correlated and Experimental Values of Dust Amount in the Feed and Products in the Laboratory Furnace. Experimental Conditions According to Table II.

Run No.	Dust Amount in the Feed (%) (experimental)	Dust Amount in the Feed (%) (correlated)	Dust Amount in the Product (%) (experimental)	Dust Amount in the Product (%) (correlated)
1	27	26	20	19
2	27	26	35	37
3	27	26	33	30
4	27	26	32	30
5	1	1	13	13
6	1	1	25	23
7	1	1	14	13
8	1	1	27	25
9	0	0	14	13
10	0	0	20	19
11	0	0	12	11
12	0	0	21	19
13	0	0	14	15
14	0	0	16	15
15	0	0	13	12
16	0	0	19	18
17	8	7	6	6
18	8	7	15	13
19	8	7	18	17
20	8	7	24	22

parameters of the present correlations can be computed from the values of the mean size of the feed material, $\hat{x}_f$, and the oxygen-to-matte ratio, R, used in the laboratory experiments. The regression technique showed no dependency of these parameters on the oxygen concentration in the process gas, although it was varied in the experiments. This reflects the experimental results,[15] which indicated that the change in mean particle size and the amount of dust generated in the experiments were largely affected by the oxygen-to-matte ratio and the initial particle size, whereas oxygen concentration played no significant role on such responses.

A major goal of this study was to compute the amount of dust in the population of particles before and after oxidation (i.e., dust generation). In this study, any particle with size smaller than 20 μm was considered as dust,[15] regardless of its composition. The percentage of dust in a particle population was obtained by multiplying by 100 the value of the cumulative function: F_3 (x = 20 μm). The value of F_3 (x = 20 μm) was obtained by numerical integration as indicated in Equation 1.

Table IV shows the experimental and correlated values of dust in the feed and the reacted particles in the laboratory furnace. A good agreement between the correlated and the experimental values is observed in all cases. Because the uncertainty of the experimental data was about 15% of the values reported in Table IV, most of the correlated values lay within the limits of the experimental uncertainty.

It should be noted that Equation 5 was developed for particles oxidized under laboratory flash-converting conditions; thus, its applicability to an industrial flash-converting reactor may not be assured. For an industrial furnace, the numerical values of the parameters in Equation 5 may be different from those reported in Table II because there are differences in the process conditions. These include differences in the level of turbulence, residence time of the particles in the reaction shaft, and the degree of particle dispersion in the reaction chamber as a result of different burner designs. On the other hand, the net effect of the operating variables stated in Equation 6 and the general form of the correlations (Equation 5) are expected to remain unchanged because the reaction path followed by the particles is expected to be similar in both systems. Direct verification of the applicability of the correlation developed in this work to the industrial operation must await the availability of reliable data.

The agreement between the model calculations and the experimental data lay within the experimental uncertainty. The results discussed in this article suggest a potential use of the present correlation in the analysis of an industrial flash-converting reactor, including dust generation.

References

1. F.R. Jorgensen, *Proc. Australas. Inst. Min. Metall.,* 276 (1980), pp. 41–47.
2. J.G. Dunn et al., *Trans. Ins. Min. Metall.,* 102 (May-August) (1993), pp. C75–C82.
3. S. Strömberg et al., *EPD Congress 1995,* ed. G.W. Warren (Warrendale, PA: TMS, 1985), pp. 207–222.
4. S. Strömberg et al., *EPD Congress 1997,* ed. B. Mishra (Warrendale, PA: TMS, 1997), pp. 271–290.
5. R.O. Suominen et al., *Scand. J. Metall.,* 20 (1991), pp. 245–250.
6. R.O. Suominen et al., *Scand. J. Metall.,* 23 (1994), pp. 30–36.
7. K.M. Riihilahti (Licenciate Thesis, Helsinki University of Technology, Espoo, Finland, 1997).
8. Y.H. Kim and N.J. Themelis, *The Reinhardt Schuhmann International Symposium on Innovative Technology and Reactor Design in Extractive Metallurgy,* ed. D.R. Gaskell et al. (Warrendale, PA: TMS, 1986), pp. 349–369.
9. A. Jokilaakso et al., *Trans. Ins. Min. Metall.,* 100 (1991), pp. C79–C90.
10. D.B. George, R.J. Gottling, and C.J. Newman, *Copper 95-Cobre 95,* ed. W.J. Chen, C. Díaz, A. Luraschi, and P.J. Mackey. (Montreal, Canada: The Metallurgical Society of CIM, 1995), pp. 41-52.
11. A. Asteljoki et al., *Journal of Metals,* 37 (5) (1985), pp. 20–23.
12. A.A. Shook, G.G. Richards, and J.K. Brimacombe, *Metallurgical and Materials Transactions B,* 26B (1995), pp. 719–730.
13. D.M. Jones and W.G. Davenport, *EPD Congress 1996,* ed. G.W. Warren (Warrendale, PA: TMS, 1996), pp. 81–94.
14. G.J. Morgan, A.A. Shook, and J.K. Brimacombe, *Processing and Handling of Powders and Dusts,* ed. T.P. Battle and H. Henein (Warrendale, PA: TMS, 1997), pp. 161–178.
15. M. Perez-Tello et al., *Metallurgical and Materials Transactions B,* 32B (5) (2001), pp. 847–868.
16. M. Pérez-Tello, H.Y. Sohn, and P.J. Smith, *Metallurgical and Materials Transactions B,* 32B (5) (2001), pp. 869–886.
17. D. Swartling (M.S. Thesis, Royal Institute of Technology, Stockholm, 1996).
18. E.G. Kelly and D.J. Spottiswood, *Introduction to Mineral Processing* (New York: Wiley, 1982).
19. R.L. Scheaffer and J.T. McClave, *Statistics for Engineers* (Boston, MA: Duxbury Press, 1982).
20. I. Deltapoint, *DeltaGraph Pro3.5 User's Guide* (Monterey, CA: Deltapoint, 1995).
21. M. Pérez-Tello (Ph.D. Dissertation, University of Utah, 1999).

Manuel Pérez-Tello, José A. Tirado-Ochoa, and Víctor M. Sánchez-Corrales are with the Department of Chemical Engineering and Metallurgy at the University of Sonora in Mexico. Hong Yong Sohn is with the Department of Metallurgical Engineering at the University of Utah.

For more information, contact M. Pérez-Tello, University of Sonora, Department of Chemical Engineering and Metallurgy, Boulevard Luis Encinas and Rosales, Hermosillo, Sonora 83000, Mexico; +52-662-259-2107; fax +52-662-259-2107; e-mail mperezt@guayacan.uson.mx.